

A Metal–Organic Framework Containing Cationic Inorganic Layers: $\text{Pb}_2\text{F}_2[\text{C}_2\text{H}_4(\text{SO}_3)_2]$

David L. Rogow,[†] Gustavo Zapeda,[†] Claudia H. Swanson,[†] Xiaojuan Fan,[†]
Charles F. Campana,[‡] Allen G. Oliver,[†] and Scott R. J. Oliver^{*,†}

Department of Chemistry and Biochemistry, University of California, Santa Cruz, 1156 High Street,
Santa Cruz, California 95064, and Bruker AXS, Madison, Wisconsin 53711

Received May 25, 2007. Revised Manuscript Received June 22, 2007

We have discovered a metal–organic framework containing cationic inorganic layers. The metal fluoride–organodisulfonate structure, $\text{Pb}_2\text{F}_2[\text{C}_2\text{H}_4(\text{SO}_3)_2]$, was synthesized hydrothermally. The lead fluoride cationic layers are covalently connected by 1,2-ethanedisulfonate chains oriented perpendicular to the layers. The material is thermally stable to ca. 325 °C, above which the material collapses to phase-pure $\alpha\text{-PbF}_2$. This material is a rare example of the use of organosulfonates as organic linker and the first metal–organic framework to contain lead fluoride connectivity. The existence of extended cationic inorganic moieties embedded within a metal–organic framework material further diversifies the possible structure types of this rapidly growing class of materials.

Introduction

Metal–organic frameworks (MOFs) are a rapidly growing class of materials, with conference symposia recently devoted to the subject.^{1,2} The vast interest is based on their potential applications, the primary examples being gas storage,^{3–5} catalysis,^{6–8} and enantioselectivity.^{9–11} Strictly speaking, MOFs are three-dimensional networks, though lower dimensional materials frequently occur.^{12–14} In fact, the literature often refers to any dimensionality as MOFs, hybrid inorganic–organic frameworks, coordination frameworks, and even coordination polymers.^{15–17} Due to the flexibility in metal charge, coordination number, and choice of organic linker,

Table 1. Crystallographic Information, Data Collection and Refinement Parameters for SLUG-6

empirical formula	$\text{Pb}_2\text{F}_2\text{C}_2\text{H}_4\text{S}_2\text{O}_6$
formula weight	640.55
crystal size, mm	$0.16 \times 0.16 \times 0.04$
crystal system	monoclinic
space group	$C2/c$
crystal color, habit	colorless, plate
a (Å)	21.4829(10)
b (Å)	4.6185(2)
c (Å)	8.8453(4)
α (deg)	90.0
β (deg)	100.3620(10)
γ (deg)	90.0
V (Å ³)	863.31(7)
Z	4
T (K)	100(2)
D_c (mg m ^{−3})	4.928
twin ratio	0.320
μ (Mo K α) (mm ^{−1})	39.470
no. of obsd data [$I > 2\sigma(I)$]	5946
R_1 [$I > 2\sigma(I)$]	0.0587
wR_2 (all data)	0.1394
goodness of fit on F^2	1.015

* To whom correspondence should be directed. E-mail: soliver@chemistry.ucsc.edu.

[†] University of California, Santa Cruz.

[‡] Bruker AXS.

- (1) Feng, L.; Duan, X. Layered Double Hydroxides. In *Structure and Bonding*; Springer: New York, 2005; Vol. 119, pp 193–223.
- (2) Williams, G. R.; Dunbar, T. G.; Beer, A. J.; Fogg, A. M.; O'Hare, D. *J. Mater. Chem.* **2006**, *16*, 1231–1237.
- (3) Spencer, E. C.; Howard, J. A. K.; McIntyre, G. J.; Rowsell, J. L. C.; Yaghi, O. M. *Chem. Commun.* **2006**, 278–280.
- (4) Xiao, B.; Wheatley, P. S.; Zhao, X. B.; Fletcher, A. J.; Fox, S.; Rossi, A. G.; Megson, I. L.; Bordiga, S.; Regli, L.; Thomas, K. M.; Morris, R. E. *J. Am. Chem. Soc.* **2007**, *129*, 1203–1209.
- (5) Dietzel, P. D. C.; Panella, B.; Hirscher, M.; Blom, R.; Fjellvag, H. *Chem. Commun.* **2006**, 959–961.
- (6) Alaerts, L.; Seguin, E.; Poelman, H.; Thibault-Starzyk, F.; Jacobs, P. A.; De Vos, D. E. *Chem.-Eur. J.* **2006**, *12*, 7353–7363.
- (7) Guo, X. D.; Zhu, G. S.; Li, Z. Y.; Sun, F. X.; Yang, Z. H.; Qiu, S. L. *Chem. Commun.* **2006**, 3172–3174.
- (8) Evanhoe, R. *Chem. Eng. News* **2006**, *84*, 38–39.
- (9) Kesanli, B.; Lin, W. B. *Coord. Chem. Rev.* **2003**, *246*, 305–326.
- (10) Bradshaw, D.; Claridge, J. B.; Cussen, E. J.; Prior, T. J.; Rosseinsky, M. J. *Acc. Chem. Res.* **2005**, *38*, 273–282.
- (11) Lin, W. B. *J. Solid State Chem.* **2005**, *178*, 2486–2490.
- (12) Hawxwell, S. M.; Adams, H.; Brammer, L. *Acta Crystallogr. B* **2006**, *62*, 808–814.
- (13) Noro, S.; Horike, S.; Tanaka, D.; Kitagawa, S.; Akutagawa, T.; Nakamura, T. *Inorg. Chem.* **2006**, *45*, 9290–9300.
- (14) Dmitriev, A.; Spillmann, H.; Lin, N.; Barth, J. V.; Kern, K. *Angew. Chem., Int. Ed.* **2003**, *42*, 2670–2673.
- (15) Robin, A. Y.; Fromm, K. M. *Coord. Chem. Rev.* **2006**, *250*, 2127–2157.

there are now hundreds of examples, and the list continues to rapidly grow.

Despite the various terminologies, all MOFs contain metal ions coordinated by organic ligands and are frequently nanoporous. At the same time, inorganic connectivity (0D clusters to 2D layers) can occur within the structure. Control of inorganic dimensionality embedded within an MOF should have strong influence over the stability (thermal, chemical, radiative, etc.) as well as important properties such as sorption, conductivity, and magnetism. This often overlooked aspect was described and tabulated in an excellent review by Cheetham et al.¹⁶ Using their proposed nomenclature, we recently reported an “I¹O²” copper hydroxide *p*-pyridinecar-

- (16) Cheetham, A. K.; Rao, C. N. R.; Feller, R. K. *Chem. Commun.* **2006**, 4780–4795.
- (17) Liao, J. H.; Lee, T. J.; Su, C. T. *Inorg. Chem. Commun.* **2006**, *9*, 201–204.

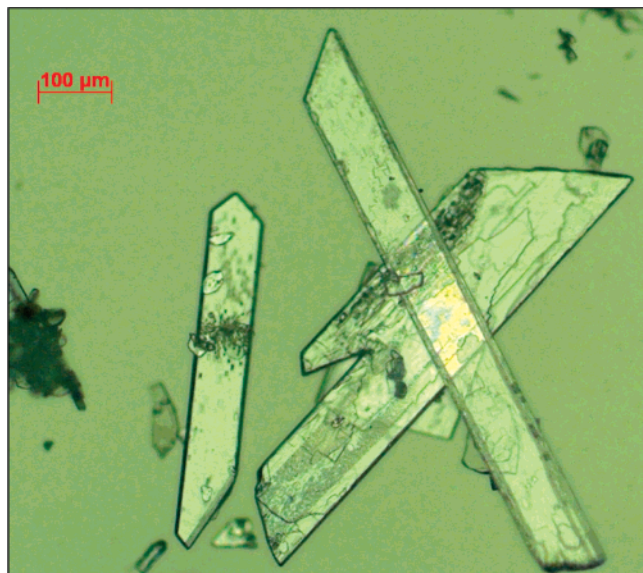


Figure 1. Optical micrograph (100 \times magnification) of the MOF crystals.

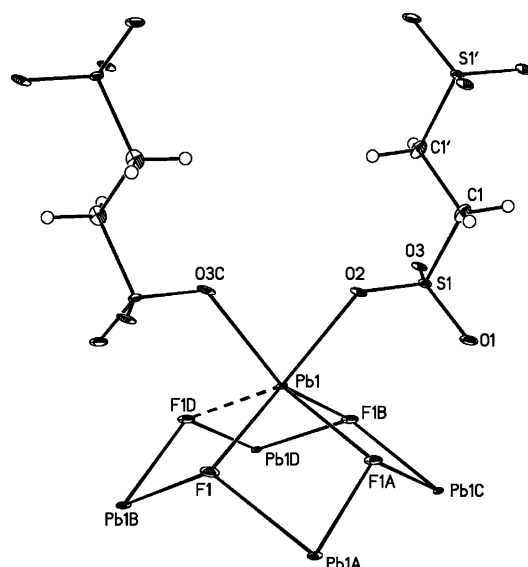


Figure 2. Atom labeling scheme, illustrating bonding and geometry around the lead center. Thermal displacement ellipsoids are shown at 50% probability.

boxylate, the first example of an MOF material with infinite 1D Cu(II) oxide chains embedded in the structure.¹⁸ Cheetham and co-workers reported a series of cobalt succinate metal–organic materials, where the inorganic connectivity and dimensionality within the MOF increased with synthesis temperature.^{16,19} Some further examples of MOFs with embedded inorganic connectivity running through the structure include neodymium oxide hydrate chains,²⁰ thorium oxyfluoride chains,²¹ and copper(I) halide chains or layers.²²

There are only two examples of extended materials to date that contain ethanedisulfonate anions. A layered double

hydroxides (LDH) type structure was reported by Cheetham and co-workers.²³ The anions are arranged parallel to the cobalt hydroxide layers and interact electrostatically. The other example consists of inorganic layers of only concatenated silver. The Ag(I) centers are covalently coordinated by the oxygen atoms of the ethanedisulfonates, and the structure may be thought of as a very early example of an MOF.²⁴ The literature as well as the Cambridge Structural Database (CSD) indicate that the remaining known ethanedisulfonate crystal structures are either inorganic clusters or simple salts. The series of metal sulfonates published by Shimizu and co-workers contain organic groups other than ethylene, and no extended inorganic connectivity beyond dimers or 1D chains are observed.²⁵ For the related class of metal phosphonates and diphosphonates (as well as those of other metals), both the phosphorus and organic group are required for structure formation, and the inorganic portion is charge neutral.²⁶

Although MOFs are well-known to have an overall cationic charge,^{21,27,28} none to date contain an extended cationic inorganic moiety. All extended inorganic moieties within the MOF are anionic or neutral in charge.¹⁶ In the course of our studies on anion templating of cationic materials,^{29–32} we discovered a layered lead fluoride where the 2D inorganic layers are cationic and covalently bonded by anionic short chain disulfonate groups.

Experimental Section

Synthesis. $\text{Pb}_2\text{F}_2[\text{C}_2\text{H}_4(\text{SO}_3)_2]$ (which we denote SLUG-6, for University of California, Santa Cruz, structure no. 6) was synthesized hydrothermally under autogenous pressure. Solid PbF_2 (ca. 5 μm powder, 99+%, Fisher Acros) and 1,2-ethanedisulfonic acid (EDSA, 95%, TCI America) were added sequentially to deionized water in a 1:2:200 molar ratio, respectively. The total volume of the reaction mixture was scaled to 10 mL and added to a Teflon-lined stainless steel autoclave (constructed in-house). The 15 mL capacity autoclave was filled to ca. $\frac{2}{3}$ volume and heated statically in an oven at 150 $^\circ\text{C}$ for 72 h. The average yield was 80%.

Instrumental. Powder X-ray diffraction (PXRD) data were recorded using a Rigaku Americas MiniFlex Plus powder diffractometer. Diffraction patterns were recorded from 4 to 60 $^\circ$ 2 θ , with a step rate of 0.04 $^\circ$ 2 θ /s. In-situ variable temperature PXRD was performed using a Rigaku Ultima III multipurpose diffraction system. Patterns were taken from 7 to 47 $^\circ$ 2 θ , with a step rate of 0.04 $^\circ$ 2 θ /s. The mounted sample was heated from 25 to 500 $^\circ\text{C}$ and powder patterns were taken at 50 $^\circ\text{C}$ intervals. Single-crystal

- (18) Tran, D. T.; Fan, X. J.; Brennan, D. P.; Zavalij, P. Y.; Oliver, S. R. *J. Inorg. Chem.* **2006**, 45, 7027–7027.
- (19) Forster, P. M.; Stock, N.; Cheetham, A. K. *Angew. Chem., Int. Ed.* **2005**, 44, 7608–7611.
- (20) Serpaggi, F.; Ferey, G. *J. Mater. Chem.* **1998**, 8, 2737–2741.
- (21) Kim, J. Y.; Norquist, A. J.; O'Hare, D. *J. Am. Chem. Soc.* **2003**, 125, 12688–12689.
- (22) Ciurtin, D. M.; Smith, M. D.; zur Loye, H. C. *Inorg. Chim. Acta* **2001**, 324, 46–56.

- (23) Forster, P. M.; Tafoya, M. M.; Cheetham, A. K. *J. Phys. Chem. Solids* **2004**, 65, 11–16.
- (24) Charbonnier, F.; Faure, R.; Loiseau, H. *Acta Crystallogr. B* **1981**, 37, 822–826.
- (25) Cote, A. P.; Shimizu, G. K. H. *Coord. Chem. Rev.* **2003**, 245, 49–64.
- (26) Miller, J. S. *ACS Symp. Ser.* **1982**, 192, 223–240.
- (27) Liu, S. X.; Xie, L. H.; Gao, B.; Zhang, C. D.; Sun, C. Y.; Li, D. H.; Su, Z. M. *Chem. Commun.* **2005**, 5023–5025.
- (28) Yang, G.; Raptis, R. G. *Chem. Commun.* **2004**, 2058–2059.
- (29) Salami, T. O.; Marouchkin, K.; Zavalij, P. Y.; Oliver, S. R. *J. Chem. Mater.* **2002**, 14, 4851–4857.
- (30) Tran, D. T.; Zavalij, P. Y.; Oliver, S. R. *J. Am. Chem. Soc.* **2002**, 124, 3966–3969.
- (31) Salami, T. O.; Fan, X.; Zavalij, P. Y.; Oliver, S. R. *J. Dalton Trans.* **2006**, 1574–1578.
- (32) Salami, T. O.; Fan, X. J.; Zavalij, P. Y.; Oliver, S. R. *J. Inorg. Chem. Commun.* **2006**, 9, 64–67.

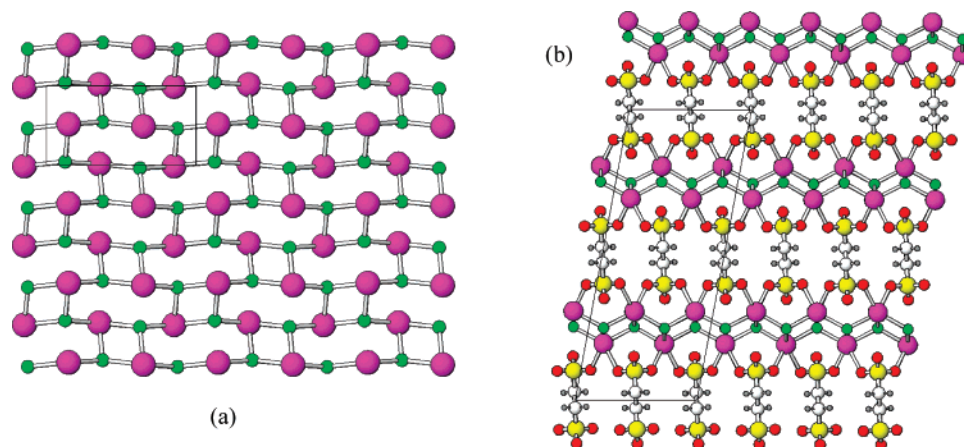


Figure 3. Crystallographic images of SLUG-6 (Pb, purple; F, green; S, yellow; O, red; C, white; H, gray). (a) View of one $[\text{Pb}_2\text{F}_2]^{2+}$ layer down the crystallographic a -axis. (b) End-on view of the layers along the crystallographic b -axis.

data were recorded using a Bruker KAPPA APEX II CCD area detector X-ray diffractometer with graphite-monochromated Mo $K\alpha$ radiation ($\lambda = 0.710\,73\text{ \AA}$). Data were collected with a combination of ω and φ scans (ω width = 0.5°) for 10 s. The data were observed to be twinned by an approximate 180° rotation about the $[001]$ direction in real space and were integrated with the appropriate twin matrix (SAINT).^{33a} The data were corrected for absorption and other effects (TWINABS).^{33b} The space group was determined to be $C2/c$ based on reflection intensities and systematic absences (XPREP).^{33c} The structure was solved by direct methods and expanded routinely from Fourier difference maps (SHELXTL).^{33d} Non-hydrogen atoms were included with anisotropic thermal motion parameters. Hydrogen atoms were included in calculated positions with thermal parameters tied to the atom to which they are bonded. Full data for the crystal structure refinement are given in Table 1.

Thermogravimetric analysis–mass spectrometry (TGA–MS) analysis was carried out using a TA Instruments 2050 thermogravimetric analyzer with $\text{N}_{2(g)}$ purge, coupled to a quadrupole sector mass spectrometer (Pfeiffer Vacuum Thermostat, GSD 301 T3) with 70 eV ionization potential. Samples were heated from ambient temperature to $600\text{ }^\circ\text{C}$ at a rate of $5\text{ }^\circ\text{C}/\text{min}$. Optical micrographs were obtained with an AxioCam MRC digital camera mounted on a Carl Zeiss Axioskop MAT optical microscope. Elemental analysis was performed by Quantitative Technologies, Inc. (Whitehouse, NJ).

Results and Discussion

The product crystals are colorless plates in a nonmerohedral twin morphology (Figure 1). The title compound forms under a wide range of synthetic conditions and starting reagent ratios. For metal to water ratios of 1:100 or less, the crystals were in the range of $30\text{--}100\text{ }\mu\text{m}$ long, and about one-third of the solid recovered was unreacted lead fluoride. More dilute conditions (from 1:150 to 1:300) resulted in larger needle-like crystals longer than $300\text{ }\mu\text{m}$ (1:200, Figure 1) and yields representative of that reported above. Synthesis temperatures higher than the ideal $150\text{ }^\circ\text{C}$ ($175\text{--}225\text{ }^\circ\text{C}$) resulted in $\alpha\text{-PbF}_2$ (ICDD # 41-1086) as the major product.

Table 2. Bond Lengths (\AA) and Angles (deg) around the Lead Center^a

Pb1–O2	2.452(6)	Pb1–F1A	2.461(4)
Pb1–F1B	2.515(4)	Pb1–O3C	2.528(6)
Pb1–F1	2.546(4)	Pb1–F1D	2.692(4)
O2–Pb1–F1A	85.79(16)	O2–Pb1–F1B	90.03(16)
F1A–Pb1–F1B	71.82(14)	O2–Pb1–O3C	75.15(17)
F1A–Pb1–O3C	138.27(15)	F1B–Pb1–O3C	143.01(14)
O2–Pb1–F1	136.86(15)	F1A–Pb1–F1	79.81(11)
F1B–Pb1–F1	122.59(16)	O3C–Pb1–F1	89.19(15)
O2–Pb1–F1D	141.21(15)	F1A–Pb1–F1D	127.29(17)
F1B–Pb1–F1D	83.51(13)	O3C–Pb1–F1D	87.37(15)
F1–Pb1–F1D	75.60(11)		

^a Symmetry transformations used to generate equivalent atoms: A, $-x + 1/2, y - 1/2, -z + 1/2$; B, $x, -y, z + 1/2$; C, $x, -y, z - 1/2$; D, $-x + 1/2, y + 1/2, -z + 1/2$.

Lower temperatures ($75\text{--}125\text{ }^\circ\text{C}$) effected no reaction of the starting lead fluoride material, which does not dissolve in water before loading into the autoclave. Therefore, $150\text{ }^\circ\text{C}$ is the ideal temperature for the solvothermal synthesis of this material with this given set of reagents and ratios. Attempts to isolate other extended structure types from this system were unsuccessful. Elemental analysis is consistent with the structural formula. Analyzed percentages of C, H, and N were 3.85%, 0.55%, and $<0.05\%$, compared with the values of 3.75%, 0.32%, and 0.00% calculated from the structure solution, respectively. The theoretical powder pattern generated from the structure solution fully matches the experimental pattern.

The structure of SLUG-6 consists of layers of lead fluoride with overall stoichiometry $[\text{Pb}_2\text{F}_2]^{2+}$ (Table 1, Figures 2 and 3a). The fluorides are triply bridging in a distorted tetrahedral geometry with one corner vacant and Pb–F–Pb bond angles of $108.18(14)^\circ$, $121.90(16)^\circ$, and $105.47(14)^\circ$. The geometry around the Pb(II) center is highly distorted five coordinate (Table 2, Figure 2). Each lead bonds to three fluorides within the layer and two interlamellar sulfonate oxygens, one for each of the two closest organosulfonates (Figure 3b). The average Pb–O distance is $2.528(6)\text{ \AA}$, well within covalent range obtained by a search of the Cambridge Structural Database (CSD; $2.604 \pm 0.211\text{ \AA}$).³⁴ The distances from oxygen O1 to the nearby symmetry-related lead Pb1 atoms are $2.880(5)$ and $2.956(5)\text{ \AA}$. These values are well beyond

(33) (a) SAINT: Software for integration of crystallographic data; Bruker Analytical X-ray Systems Inc.: Madison, WI, 2005. (b) Sheldrick, G. M. TWINABS. University of Göttingen, Germany, 2005. (c) XPREP: Part of the SHELXTL Crystal Structure Determination Package, 5.03; Siemens Industrial Automation, Inc.: Madison, WI, 1995. (d) SHELXTL Crystal Structure Determination Package; Bruker Analytical X-ray Systems Inc.: Madison, WI, 1995–99.

(34) Allen, F. H. *Acta Crystallogr. B* **2002**, 380–388.

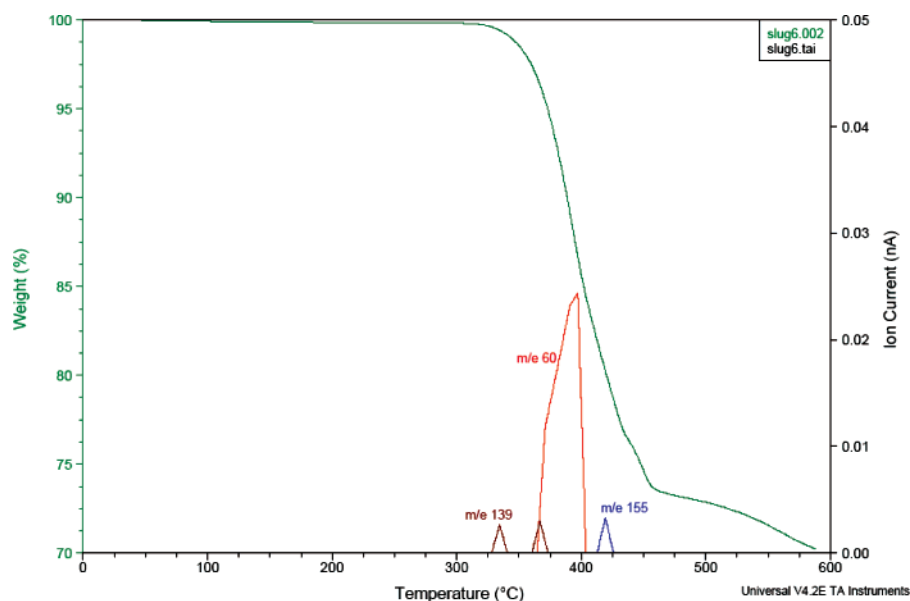


Figure 4. TGA–MS shows the material is stable to ca. 325 °C, with fragments of ethanedisulfonate evolved during the decomposition to $\alpha\text{-PbF}_2$.

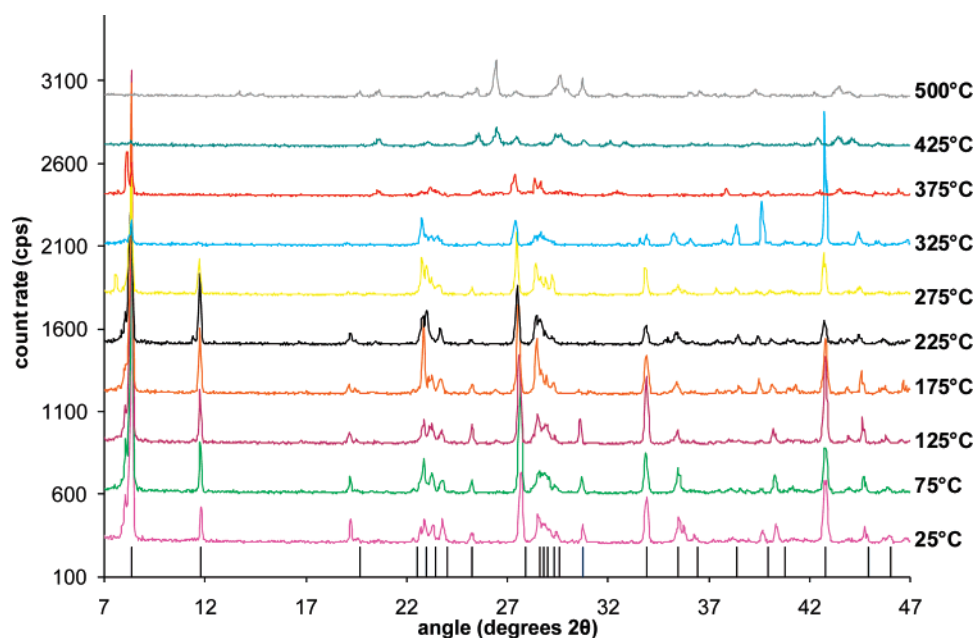


Figure 5. In situ variable-temperature PXRD, with the theoretical pattern shown at the bottom. The pattern at 425 °C and above indexes to $\alpha\text{-PbF}_2$.

reasonable bonding distances. A long Pb–F contact [2.692–(4) Å] to a fourth fluoride center also exists on each Pb center (dashed line, Figure 2). The lone pair on the Pb(II) center is likely oriented along this bond and therefore points into the rectangle-like gaps (Figure 3a). The anionic ethanedisulfonate $[\text{C}_2\text{H}_4(\text{SO}_3)_2]^{2-}$ molecules reside between the layers, aligned perpendicular to the lead fluoride sheets (Figure 3b).

This topology is a rare example of a 2D cationic inorganic motif. The only previous examples are the LDHs (a widely studied isostructural set also known as hydrotalcites)^{35,36} and our previously reported $\text{Pb}_3\text{F}_5\text{NO}_3$.³⁰ The overall structure,

however, is a covalent 3D MOF rather than a cationic layer, since the ethanedisulfonate molecules are anchored to the Pb centers. Indeed, attempts to remove or exchange the organic anions from the host structure while leaving the cationic layers intact have thus far been unsuccessful. We attempted to exchange the ethanedisulfonate anions for benzoate and permanganate in aqueous solution, neither of which gave any change in the PXRD pattern for the resultant solid. As outlined above, our material is also a rare example of an inorganic material containing ethanedisulfonate.^{23,24}

A search of the CSD shows only four known organic structures containing Pb–F bonds, and all are molecular. There are two-dimensional lower p-block metal oxides known, such as the Aurivillius phases,³⁷ though these are

(35) Evans, D. G.; Slade, R. C. T. *Layered Double Hydroxides*. In *Structure and Bonding*; Springer: New York, 2005; Vol. 119, pp 1–87.

(36) He, J.; Wei, M.; Li, B.; Kang, Y.; Evans, D. G.; Duan, X. *Layered Double Hydroxides*. In *Structure and Bonding*; Springer: New York, 2005; Vol. 119, pp 89–119.

(37) Sharma, N.; Linga, C. D.; Wrighter, G. E.; Chena, P. Y.; Kennedy, B. J.; Lee, P. L. *J. Solid State Chem.* **2007**, *180*, 370–376.

high-temperature, highly condensed defect perovskite-type structures. Red lead (α -PbO, the mineral known as litharge)³⁸ has the inert pair of the metal pointing into the interlamellar space, whereas in our case, the structure is a metal fluoride and the lone pair is oriented parallel to the layer. The structure, however, is closely related to grandreefite, an entirely inorganic material with formula $\text{Pb}_2\text{F}_2\text{SO}_4$.³⁹ The lead fluoride layers have the same connectivity as SLUG-6, but with direct connection via the sulfates as well as Pb–O–Pb bonds. The bonding distances and unit cell dimensions for grandreefite are therefore shorter, both within and between the layers. Thus, the mineral structure can be considered a highly condensed 3D framework rather than a pillared 2D material.

TGA–MS data shows the thermal stability of the material to ca. 325 °C (Figure 4). The mass spectrum shows fragments corresponding to mercaptan and organosulfonate fragments of ethanedisulfonate. Mass fragments of 155 and 139 m/z correspond to $\text{O}_2\text{SCH}_2\text{CH}_2\text{SO}_2$ and $\text{OSCH}_2\text{CH}_2\text{SO}_2$, respectively. The 60 m/z fragment observed is most likely the $-\text{CH}_2\text{CH}_2\text{S}-$ fragment of ethanedisulfonate. The theoretical weight loss upon collapse of the layers and calcination of the organic ethanedisulfonate molecules is 29%. This is consistent with the TGA trace in Figure 4, where it is shown that $\sim 70\%$ of the starting mass remains upon full calcination of the ethanedisulfonate molecules. Upon heating past 500 °C, the material collapses to α -PbF₂, as evidenced by ex-situ heating to 700 °C and subsequent PXRD measure-

ment. In-situ variable-temperature PXRD further confirms the thermal stability of the material (Figure 5). The interlamellar organic groups begin to decompose at approximately 325 °C. The material collapses to phase-pure α -PbF₂ by 425 °C.

Conclusions

This is the only example to date of an MOF material containing a cationic inorganic covalent network. A multitude of new structures should be possible by varying the organic group that connects the two sulfonate groups. Attempts to date with propylenedisulfonate as either structure-directing agent or anion-exchange source have not been successful. It may be possible to tune the coordinating strength of the sulfonate, for example, with a perfluorinated carbon chain, thereby preventing covalent bond formation to the cationic layers. Discrete anions that only interact electrostatically with the inorganic layers are necessary for our target applications of base catalysis and environmental remediation. We have had success in this regard with ethanedisulfonate and other lower p-block metals, as we will soon report. We are also currently studying other mono- and oligosulfonates to template the extended structure.

Acknowledgment. This research was supported by an NSF Career Award (DMR-0506279). The single crystal X-ray diffraction data in this work were recorded on an instrument supported by the NSF Major Research Instrumentation (MRI) Program under Grant No. CHE-0521569. We thank Dr. Akhilesh Tripathi of Rigaku Americas, Inc. for variable-temperature PXRD measurements.

Supporting Information Available: Crystallographic information file (CIF) containing refinement parameters, fractional atomic coordinates, and bond lengths and angles. This material is available free of charge via the Internet at <http://pubs.acs.org>.

CM071429T

(38) Boden, D. P. *J. Power Sources* **1998**, 73, 56–59.

(39) Kampf, A. R. *Am. Mineral.* **1991**, 76, 278–282.